Ocean heat storage rate unaffected by MOC weakening in an idealised climate model

Peter Shatwell[1], Arnaud Czaja[2], and David Ferreira[3]

[1]Imperial College London
[2]Imperial College, Dept. Physics
[3]University of Reading

November 26, 2022

Abstract

To study the role of the Atlantic meridional overturning circulation (AMOC) in climate change, we perform an abrupt CO2-doubling experiment using a coupled atmosphere-ocean-ice model with a simple geometry that separates the ocean into small and large basins. As in observations and high-end climate models, the small basin exhibits a MOC and warms at a faster rate than the large basin. In our set-up, this contrast in heat storage rates is 0.6 +/- 0.1 W/m^2, and we argue that this is due to the small basin MOC. However, the MOC weakens significantly, yet this has little impact on the small basin's heat storage rate. We find this is due to the effects of both compensating warming patterns and interbasin heat transports. Thus, although the presence of a MOC is important for enhanced heat storage, MOC weakening is surprisingly unimportant.

Ocean heat storage rate unaffected by MOC weakening in an idealised climate model

Peter Shatwell[1], **Arnaud Czaja**[1], **David Ferreira**[2]

[1]Department of Physics, Imperial College London
[2]Department of Meteorology, University of Reading

Key Points:

- A deep MOC connects the ocean surface to its interior and enhances heat storage rate under global warming
- The AMOC may give the Atlantic its enhanced heat storage rate relative to the Pacific in recent decades
- MOC weakening has little impact on ocean heat storage rate due to compensating physical processes

Corresponding author: Peter Shatwell, `peter.s@imperial.ac.uk`

Abstract

To study the role of the Atlantic meridional overturning circulation (AMOC) in climate change, we perform an abrupt CO_2-doubling experiment using a coupled atmosphere-ocean-ice model with a simple geometry that separates the ocean into small and large basins. As in observations and high-end climate models, the small basin exhibits a MOC and warms at a faster rate than the large basin. In our set-up, this contrast in heat storage rates is 0.6 ± 0.1 W m^{-2}, and we argue that this is due to the small basin MOC. However, the MOC weakens significantly, yet this has little impact on the small basin's heat storage rate. We find this is due to the effects of both compensating warming patterns and interbasin heat transports. Thus, although the presence of a MOC is important for enhanced heat storage, MOC weakening is surprisingly unimportant.

Plain Language Summary

The oceans take up the vast majority of the excess heat energy due to global warming. One of the most important large-scale ocean circulations is the Atlantic meridional overturning circulation (AMOC). Under global warming, it's been suggested that this circulation is important for capturing and storing heat energy in the deep ocean. In order to examine this process more closely, we use a simple computer model of a world with no land masses and only two ocean basins: a small basin with a circulation similar to the AMOC, and a large basin without. We mimic global warming by increasing the CO_2 in the model atmosphere, and we find that the small basin warms at a faster rate than the large basin. In observations, the AMOC has weakened since the mid-twentieth century, and some worry that surface warming will intensify in response to the Atlantic storing less heat energy in the deep ocean. In our experiment, the overturning circulation does weaken, but this weakening does not affect the heat storage rate in the small basin. This is a surprising result and casts doubt on the concern that a weaker AMOC will lead to rapid surface warming in Earth's future climate.

1 Introduction

Due to anthropogenic carbon emissions, there is now greater absorbed solar radiation than outgoing long-wave radiation over the surface of the Earth, leading to a positive imbalance, designated Earth's energy imbalance (EEI) (Von Schuckmann et al., 2016; Trenberth et al., 2014; Hansen et al., 2011). The vast majority ($\sim$93%) of the excess energy resulting from this imbalance manifests as an increase in ocean heat content (OHC) (Stocker, 2014), and improving estimates of OHC has been highlighted as critical to constraining EEI and thus understanding Earth's heat storage (Von Schuckmann et al., 2016).

Ocean heat uptake (OHU) acts as a buffer for surface warming. If more energy is taken into the ocean interior, then less is absorbed at the atmospheric surface; indeed, so-called 'surface warming hiatuses' have been linked to periods of enhanced ocean heat uptake (Drijfhout et al., 2014; Watanabe et al., 2013; Meehl et al., 2011). Recently, more attention has been drawn to the role of ocean circulation on heat uptake (e.g. Marshall et al. (2015); Winton et al. (2013)), particularly that of the Atlantic's meridional overturning circulation (AMOC). It is possible that the presence of this circulation gives the Atlantic its enhanced warming rate compared to the Pacific, as seen in observations (e.g. Chen and Tung (2014); Desbruyeres et al. (2017); Zanna et al. (2019)).

The depth and strength of the AMOC positively correlates with the depth of global ocean heat storage (OHS) across models participating in the fifth phase of the Coupled Model Intercomparison Project (CMIP5) (Kostov et al., 2014), and its multidecadal variability has been linked to periods of enhanced global surface warming and cooling (Chen & Tung, 2018). The AMOC's role in global OHS is especially interesting due to the possibility of it weakening in the future. A robust weakening response of the AMOC with global surface warming ($\sim$0.05 Sv per year) is seen across CMIP5 models (Weaver et al., 2012), and observations point to the AMOC having weakened since the mid-twentieth century (Caesar et al., 2018). Model biases may favour a stable AMOC, and it is still a concern that the AMOC could collapse in the future, leading to abrupt changes in climate (Caesar et al., 2018; Liu et al., 2017).

A weakening AMOC results in a weakening of the northward oceanic meridional heat transport (MHT), which could explain the conspicuous region of cooling in the subpolar North Atlantic found in maps of temperature trends (Rahmstorf et al., 2015). It's been suggested that this North Atlantic surface cooling reduces the sea-air temperature difference, and so reduces the sensible heat flux from the ocean to the atmosphere i.e. an increase in ocean heat uptake (Drijfhout et al., 2014; Winton et al., 2013).

This appears to be at odds with the idea that a deeper and stronger AMOC results in more global ocean heat storage (Kostov et al., 2014). However, this inconsistency may disappear if we clarify the distinction between *uptake* and *storage*. Over an ocean column, a change in OHC is due to the net air-sea heat flux $\mathcal{F}_s$ (W m^{-2}) as well as the heat transport into or out of the column:

$$\partial_t \int_{-H}^{0} \rho_0 c_p \theta \, dz = \mathcal{F}_s - \rho_0 c_p \int_{-H}^{0} \nabla \cdot (\mathbf{v}\theta) \, dz \tag{1}$$

where θ is the oceanic potential temperature, ρ_0 the seawater density, and c_p the specific heat capacity of seawater. Heat uptake is synonymous only with $\mathcal{F}_s$ (i.e. heat penetrating the ocean surface), while heat storage refers to an increase in OHC (l.h.s. of equation 1). Thus, OHU and OHS can be very different regionally due to the ocean heat transport divergence $\nabla\cdot(\mathbf{v}\theta)$. Only globally are they equivalent, when this divergence term vanishes. Thus, it's possible that a weaker AMOC can cause an increase in heat uptake regionally at the same time as a decrease in heat storage globally.

Recent work (Saenko et al., 2018) has cast doubt on the observed model correlation between AMOC strength and heat storage (Kostov et al., 2014), suggesting that the eddy parameterisation affects both AMOC strength and global OHU efficiency, thus causing a spurious correlation between the two quantities. But without a better conceptual grasp on how the AMOC affects OHS, it is unclear whether this correlation is spurious or not. Furthermore, these studies (Saenko et al., 2018; Kostov et al., 2014) establish a link between the AMOC and *global* OHS, while it may be easier to first consider the AMOC's influence on heat storage within the Atlantic basin itself. Given the importance of constraining and monitoring EEI through OHC observations, and the possibility that the AMOC may continue to weaken into the future, it is imperative to better understand the AMOC's role in ocean heat uptake and storage as the world continues to warm.

To this end, we examine the response of a coupled atmosphere-ocean-ice general circulation model under an abrupt doubling of atmospheric CO_2. The model geometry invokes two sea-floor to sea-surface meridional barriers that separate the ocean into small and large basins. The small basin exhibits an overturning circulation akin to the AMOC, while the large basin does not. We look at the basins' individual responses rather than taking a global perspective, and we isolate the effect of the small basin MOC by focusing on small–large basin differences. We describe the model formulation and geometry in section 2. In section 3, we present results from the abrupt CO_2-doubling experiment where we find and define a heat storage contrast between the small and large basins, and explore the role of the small basin's MOC in establishing this contrast. A discussion is given in section 4, and we conclude in section 5.

2 Model Description and Set-up

The model uses the Massachusetts Institute of Technology general circulation model (MITgcm) code (Marshall, Adcroft, et al., 1997; Marshall, Hill, et al., 1997). Both the atmosphere and ocean component models use the same cubed-sphere grid at a C24 resolution (24x24 points per face, giving a resolution of 3.75° at the equator). The atmosphere has a low vertical resolution of five levels, and its physics is based on the 'simplified parameterisations primitive-equation dynamics' (SPEEDY) scheme (Molteni, 2003). The ocean is flat-bottomed with a constant depth of 3 km, and is split into 15 levels with increasing vertical resolution from 30 m at the surface to 400 m at depth.

Mesoscale eddies are parameterised as an advective process (Gent & Mcwilliams, 1990) and an isopycnal diffusion (Redi, 1982), both with a transfer coefficient of 1200 $m^2\ s^{-1}$. Ocean convection is represented by an enhanced vertical mixing of temperature and salinity (Klinger et al., 1996), while the background vertical diffusion is uniform and set to $3 \times 10^{-5}\ m^2\ s^{-1}$. There are no sea-ice dynamics, but a simple two and a half layer thermodynamic sea-ice model (Winton, 2000) is incorporated. The seasonal cycle is represented, but there is no diurnal cycle.

The model is configured with the idealised 'Double-Drake' (DDrake) geometry as seen in previous work (e.g. Ferreira et al. (2010, 2015); Ferreira and Marshall (2015)), which is an aquaplanet with two narrow vertical barriers that extend from the sea floor to the sea surface. The barriers are set 90° apart at the North Pole and extend meridionally to 35°S. This separates the ocean into small and large basins, with both of them connected by a 'southern ocean' region south of 35°S. The small and large basins in this configuration exhibit distinctive Atlantic-like and Pacific-like characteristics, with the small basin being warmer and saltier, and exhibiting a deep interhemispheric MOC (see figure S1 in supporting information). The model geometry captures two important asymmetries relevant to the Earth's climate: a zonal asymmetry splitting the ocean into small and large basins, and a meridional asymmetry allowing for circumpolar flow in the Southern Hemisphere, but not in the Northern Hemisphere.

The model is spun up for 6000 years until a statistically steady state is reached. The time-mean of the last 50-year integration is used as the equilibrated control climate state. We abruptly change the longwave absorption in the CO_2 band, causing an initial top-of-atmosphere forcing (EEI) of approximately 3.7 W m^{-2}, thus mimicking an abrupt doubling of atmospheric CO_2 (Myhre et al., 1998), and run for an additional 200 years. The imposed EEI results in a warming of the climate system, and we diagnose the ensuing responses of the small and large basins relative to the control climate.

3 Results

3.1 Heat Storage Rates

The small basin (SB) warms at a faster rate than the large basin (LB) (figure 1a). The large basin's surface area is three times larger than that of the small basin, yet it only takes up 2.21 times more heat energy in joules over the course of the simulation. By considering areal proportions of the total global OHC increase, we find that this is due to a combination of the SB taking up more heat than expected for its size, and the LB taking up less than expected (see figure S2 in supporting information).

To compare the two basins' efficiencies in storing heat, we look at basin OHC changes divided by the respective basin's surface area (in J m^{-2}). We use Δs to represent changes to quantities due to the abrupt CO_2-doubling. After 200 years' warming, the final anomalous OHC difference, $\Delta OHC_{SB} - \Delta OHC_{LB}$, is 3.45×10^9 J m^{-2} (figure 1b), and in terms of heat storage *rates* in W m^{-2}, this translates to a time-mean heat storage contrast of 0.6 ± 0.1 W m^{-2} (figure 1c). There is large interannual variability in the heat storage rates, and the heat storage contrast shows no discernible trend over the 200 years. At the same time, we see that the SB MOC strength weakens rapidly by ~25% during the first 30 years (figure 1d), after which it remains quite stable between 18 and 20 Sv (1 Sv $\equiv 10^6$ m^3 s^{-1}).

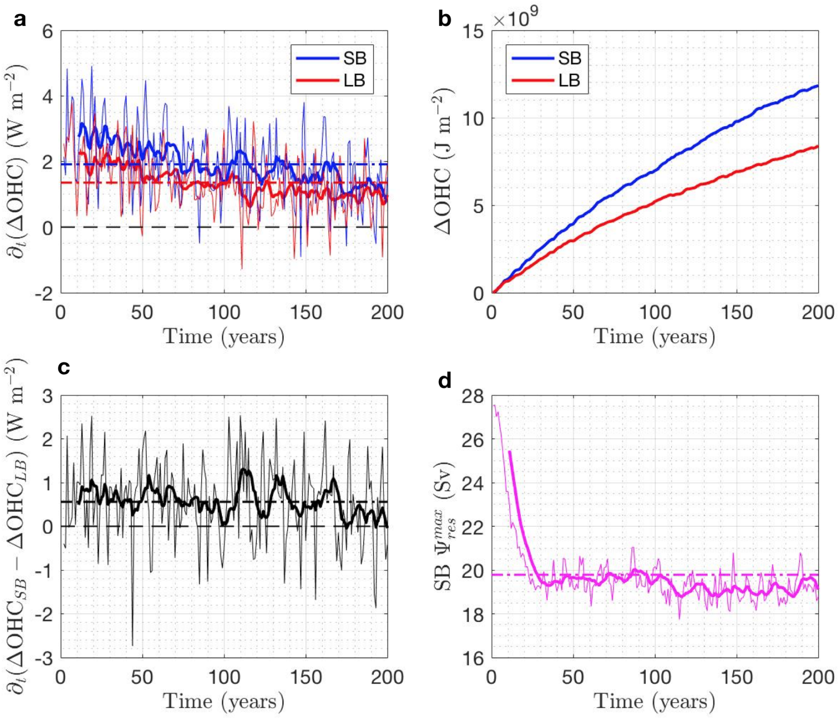

Figure 1. Time series of (a) SB and LB heat storage rates; (b) OHC anomalies; (c) the difference in heat storage rates i.e. the heat storage contrast; and (d) SB MOC strength following an abrupt doubling of CO_2. Thick lines are decadal running means and horizontal dash-dot lines indicate time-mean values. The time-mean heat storage contrast is 0.6 ± 0.1 W m^{-2} (standard error).

3.2 Role of the Small Basin MOC

To make the connection with the SB MOC, we look at the spatial pattern of the vertically-averaged potential temperature response $\Delta\theta$ for different depth intervals (figure 2a, b). The upper 1 km reveals pronounced warming at high latitudes, a conspicuous pool of warming at 40-60°N in the SB, and enhanced warming at 40°S where there is zonal circumpolar flow, reminiscent of warming behaviour along the Antarctic Circumpolar Current (ACC) (Armour et al., 2016). Below 1 km depth, the temperature anomaly in the SB appears to flow along a deep western boundary current, coincident with the lower limb of its MOC. Note there are no large temperature anomalies at depth in the LB or southern ocean regions.

The MOC's role is made even clearer when we plot the control residual overturning (Ψ_{res}^{ctrl}) on top of the final zonally-averaged $\Delta\theta$ in the SB (figure 2c). There is a distinctive convective chimney at 60-80°N, collocated with the downwelling branch of Ψ_{res}^{ctrl}. The $\Delta\theta$ structure also approximates the pattern of the streamlines, and we see an isolated pool of warm water between 1 and 1.5 km depth near the equator, suggesting the equatorward advection of temperature anomalies into this region away from the high latitudes of deep water formation.

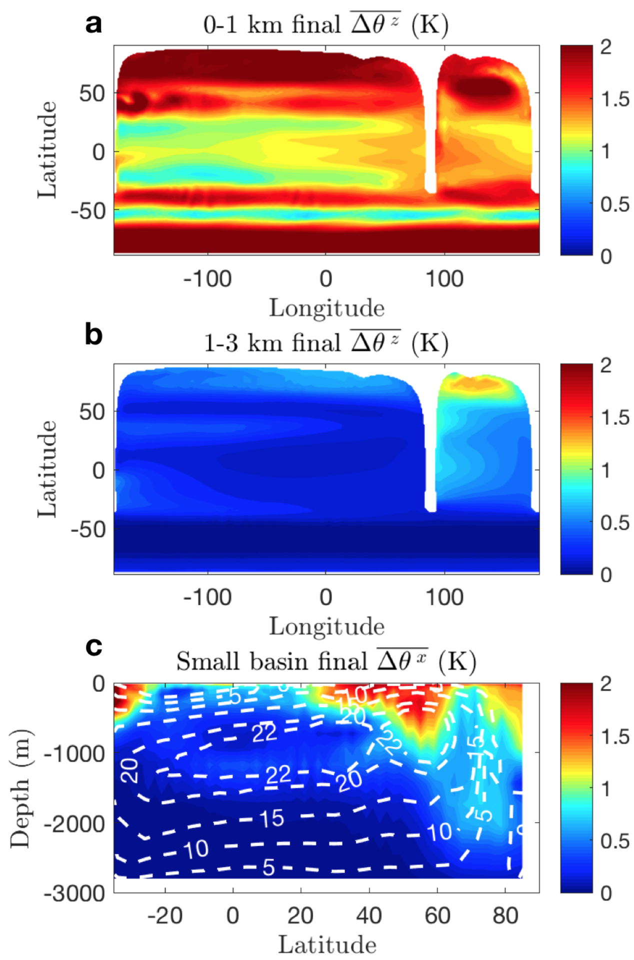

Figure 2. Vertically-averaged $\Delta\theta$ (in K) after 200 years following an abrupt doubling of atmospheric CO_2 in DDrake for the depth intervals (a) 0-1 km and (b) 1-3 km. The temperature anomaly at depth follows a deep western boundary current in the small basin. (c) Zonally-averaged $\Delta\theta$ (colour, in K) in the small basin after 200 years' warming, and streamlines (white dashed contours, in Sv) for the control residual overturning Ψ_{res}^{ctrl}.

3.3 MOC Weakening

From the previous section, it is clear that the SB MOC plays an important role in setting the heat storage contrast between the two basins of DDrake. However, the SB MOC strength weakens rapidly by ∼25% during the first 30 years, after which it remains stable between 18 and 20 Sv (figure 1d). The heat storage contrast remains approximately constant over the 200 years (figure 1c), so we find that this MOC weakening has little, if any, impact on the heat storage contrast.

To explain this, consider the vertical heat flux associated with the SB MOC, approximated by $\rho_0 c_p \Psi_{res} \delta\theta$ (in W), where $\delta\theta$ is the temperature difference across the downwelling and upwelling branches of the circulation i.e. $\theta_\downarrow - \theta_\uparrow$. We take vertically-averaged θ values in the latitude bands 60-80°N and 30-50°S in the SB sector for $\theta_\downarrow$ and $\theta_\uparrow$, respectively. Considering orders of magnitude, $\rho_0 = 1030$ kg m^{-3}, $c_p = 3994$ J kg^{-1} K^{-1}, $\Psi_{res} \sim \mathcal{O}(10^7)$ m^3 s^{-1}, and $\delta\theta \sim \mathcal{O}(1)$ K. Together, these estimates give a scaling of $\sim \mathcal{O}(10^{13})$ W. As the SB surface area is $\sim \mathcal{O}(10^{13})$ m^2, we find that the heat flux due to the SB MOC should be $\sim \mathcal{O}(1)$ W m^{-2}, which is the same order as the heat storage contrast found in figure 1c.

Following the CO_2-doubling, we must consider the change in the MOC heat flux, $\Delta\mathcal{H}_{MOC} = \rho_0 c_p \Delta(\Psi_{res}\delta\theta)$. Let overlines represent time-mean quantities in the control integration. (Again, Δs represent changes to quantities due to the CO_2-doubling.) A change in the MOC heat flux (divided by $\rho_0 c_p$) is then:

$$\Delta(\Psi_{res}\delta\theta) = \underbrace{\Delta\Psi_{res}\overline{\delta\theta}}_{>0} + \underbrace{\overline{\Psi_{res}}\Delta(\delta\theta)}_{>0} + \underbrace{\Delta\Psi_{res}\Delta(\delta\theta)}_{<0} \; > \; 0 \tag{2}$$

where we take the convention that a downward heat flux is positive. There are two processes to consider: one due to $\Delta\Psi_{res}$ (MOC weakening) and one due to $\Delta(\delta\theta)$ (differential warming). We find that $\theta_\downarrow$ warms at a faster rate than $\theta_\uparrow$, so that $\Delta(\delta\theta) > 0$ (see figure S3 in supporting information). The second term in equation 2 is then positive, leading to an increase in the anomalous downward heat flux.

Now, we know that the MOC weakens ($\Delta\Psi_{res} < 0$), so one might think that this process compensates the differential warming (as $\Delta(\delta\theta) > 0$). Importantly, however, in the control integration, $\overline{\delta\theta} = -0.7$ K (< 0), indicating that the MOC is thermally direct and transports heat *upwards*. So, the first term in equation 2 is in fact *positive*. Both the differential warming *and* the MOC weakening processes contribute to an *increase* in the anomalous downward heat flux. Only their interaction $\Delta\Psi_{res}\Delta(\delta\theta)$ is negative, leading to an upward heat flux. These terms are plotted (in W m^{-2}) in figure 3a. Notably, the two terms involving $\Delta\Psi_{res}$ (i.e. MOC weakening) compensate each other, while the dominant term is $\overline{\Psi_{res}}\Delta(\delta\theta)$, so the control overturning is still playing a prominent role.

The anomalous downward MOC heat flux thus increases with time, and most rapidly during the MOC weakening. Why this increase in $\Delta\mathcal{H}_{MOC}$ does not lead to an increase in the heat storage contrast remains to be explained. If we consider the air-sea heat flux (heat uptake) compared to the increase in OHC (heat storage) in the small basin, we find that the small basin *leaks heat* across 35°S to the southern ocean region at a rate of ~0.5 W m^{-2}, and this leakage rate increases with time (figure 3b).

Recall equation 1. For an increase in OHC in the small basin, we can write

$$\partial_t(\Delta OHC_{SB}) = \mathcal{F}_s^{SB} - \rho_0 c_p \int_{-H_{SB}}^{0} \nabla \cdot (\Delta(\mathbf{v}\theta_{SB}))\, dz = \mathcal{F}_s^{SB} + \Delta\mathcal{H}_{leak} \tag{3}$$

where we define $-\rho_0 c_p \int_{-H_{SB}}^{0} \nabla \cdot (\Delta(\mathbf{v}\theta_{SB}))\, dz = \Delta\mathcal{H}_{leak}$ as the SB heat leakage rate across 35°S. From figure 3b, we see that $\Delta\mathcal{H}_{leak}$ and $\Delta\mathcal{H}_{MOC}$ compensate each other, especially on long timescales (see dashed lines). This is made even clearer in an energy budget sense, where we find that $\partial_t(\Delta OHC_{SB}) + \Delta\mathcal{H}_{MOC} \approx \mathcal{F}_s^{SB}$ (light blue, dashed), which implies that $\Delta\mathcal{H}_{MOC} \approx -\Delta\mathcal{H}_{leak}$. So, as the SB MOC heat flux increases, this permits more heat to penetrate the ocean surface, causing an increase in the surface heat flux $\mathcal{F}_s^{SB}$. However, this additional heat input is then lost to the southern ocean, which ensures that the heat storage contrast remains stationary.

4 Discussion

The key process governing the enhanced heat storage rate in the SB is the rapid subduction of surface temperature anomalies into the interior associated with its MOC. We acknowledge that this relies on an implicit connection between deep convection and

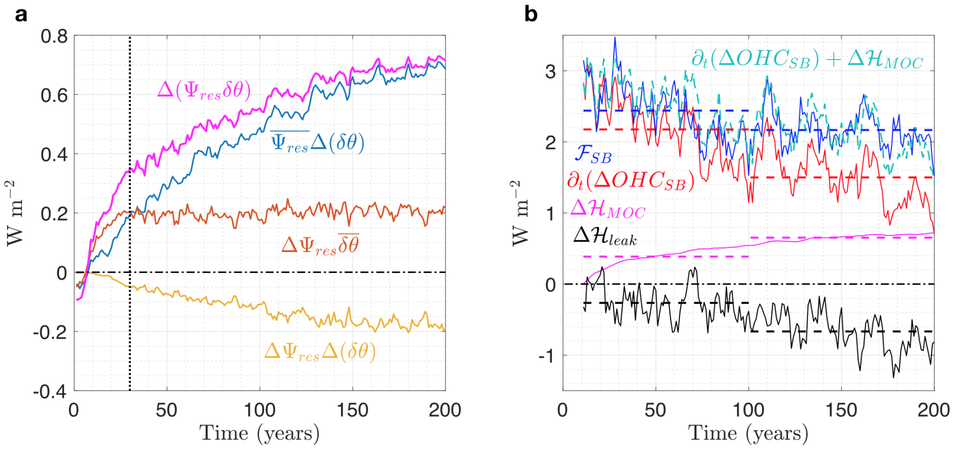

Figure 3. (a) Decomposition of the change in SB downward (positive) MOC heat flux ($\Delta(\Psi_{res}\delta\theta)$, magenta) into differential warming ($\overline{\Psi_{res}}\Delta(\delta\theta)$, blue), MOC weakening ($\Delta\Psi_{res}\overline{\delta\theta}$, orange), and nonlinear ($\Delta\Psi_{res}\Delta(\delta\theta)$, yellow) terms (in W m^{-2}). A vertical dotted line is plotted at 30 years to separate the weakening and non-weakening MOC regimes. (b) Decadal running means of the SB heat uptake rate ($\mathcal{F}_s^{SB}$, blue), heat storage rate ($\partial_t(\Delta OHC_{SB})$, red), MOC heat flux ($\Delta\mathcal{H}_{MOC}$, magenta), and leakage rate to the southern ocean ($\Delta\mathcal{H}_{leak} = \partial_t(\Delta OHC_{SB}) - \mathcal{F}_s^{SB}$, black) (in W m^{-2}). Note that the sum of the heat storage rate and MOC heat flux (light blue, dashed) almost matches the heat uptake rate. Horizontal dashed lines are centennial time-means.

a MOC, which is perhaps an oversimplification as the relationships between deep water formation and overturning are complex and remain unclear (Straneo, 2006; M. S. Lozier, 2012). Nevertheless, the centrality of the SB MOC for its enhanced heat storage rate highlights the importance of the present-climate AMOC, which could help explain the Atlantic's observed enhanced warming rate compared to the Pacific (Chen & Tung, 2014; Desbruyeres et al., 2017; Zanna et al., 2019).

Weakening of the AMOC has been seen in observations and climate models (Rahmstorf et al., 2015; Srokosz & Bryden, 2015; Caesar et al., 2018; Weaver et al., 2012; Gregory et al., 2005), and it has been suggested that a continued weakening in the future could lead to a loss of this deep ocean heat storage mechanism, resulting in an accelerated warming of surface temperatures (Chen & Tung, 2018). However, we think this view focuses too narrowly on $\Delta\Psi_{res}$ and, as we have found in our experiments, considering $\Delta(\Psi_{res}\delta\theta)$ paints a more complicated picture.

Our explanation of the constancy of the SB/LB heat storage contrast relies on a southward transport of heat from the small basin to the southern ocean region of DDrake. This is similar to the 'redistribution temperature' response seen in Xie and Vallis (2012) where, in an idealised model of the Atlantic ocean, the MOC weakening serves to transport heat from the Northern Hemisphere high latitudes towards the Southern Hemisphere. However, we note that across CMIP5 models, the Southern Ocean dominates ocean heat uptake and exports approximately half of the energy it takes up *northwards* (Frölicher et al., 2015); this northward transport is also supported by observations, which results in a delayed warming of the Southern Ocean (Armour et al., 2016). We suspect that the circumpolar-average picture in these studies obscures a southward transport from the Atlantic basin to the Southern Ocean.

Nevertheless, our analysis paves a way towards understanding the AMOC's role in ocean heat storage in observations and more complicated climate models. A preliminary look at four CMIP5 models shows that there is a heat storage contrast between the Atlantic and Pacific basins (defined from 30°S to 65°N) in abrupt CO_2-quadrupling experiments (figure 4). Under this more intense forcing scenario, the multi-model time-mean heat storage contrast is 2.2 W m^{-2}. Looking at individual models, the contrast persists in the models CANESM2 and NASA-GISS-E2-H, but closes in MIROC-ESM and GFDL-ESM2M. This could be due to different model AMOC responses and, particularly, whether the control model AMOC cells are thermally direct (flux heat upward, like the SB MOC) or indirect (flux heat downward), but warrants further study. For example, Zika et al. (2013) diagnosed overturning cells in UVic ESM and found that the cell coincident with the AMOC was thermally indirect, so our results might not apply to this model. In any case, we suggest that the AMOC is at least responsible for the existence of a contrast in each of these CMIP5 models, just as the SB MOC is responsible for the contrast in DDrake.

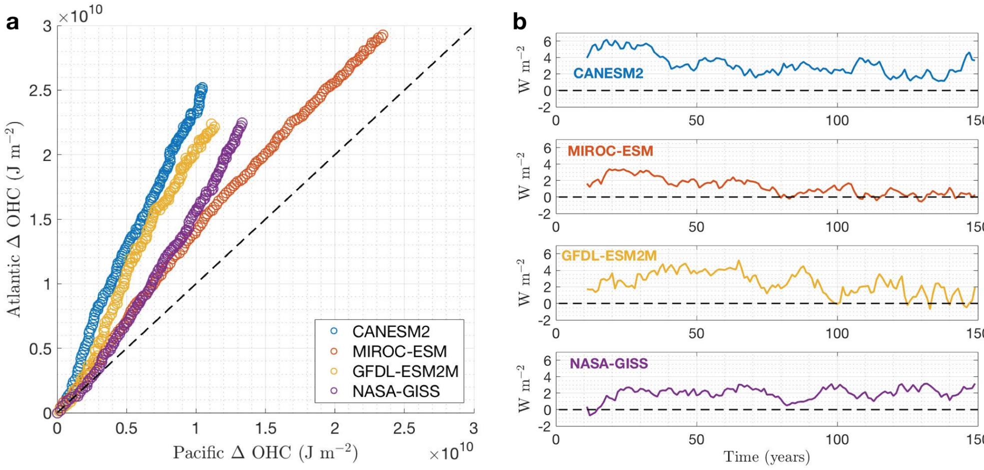

Figure 4. (a) Atlantic vs. Pacific top-3 km column-averaged annual OHC anomalies (in J m^{-2}) following an abrupt quadrupling of atmospheric CO_2 in CMIP5 models. Atlantic and Pacific basins defined from 30°S to 65°N. The deviation from the identity line (black dashed) highlights the Atlantic's enhanced warming rate relative to the Pacific in these experiments. (b) Decadal running means of individual model Atlantic–Pacific heat storage contrasts $\partial_t(\Delta OHC_{Atl} - \Delta OHC_{Pac})$ (in W m^{-2}).

5 Conclusion

Using an idealised coupled climate model under an abrupt doubling of atmospheric CO_2, we have shown that an ocean basin endowed with a MOC experiences an enhanced heat storage rate due to a rapid subduction of surface temperature anomalies into its interior. Similar to Kostov et al. (2014), who found no significant correlations between the AMOC weakening and the depth of heat storage in CMIP5 models, we find no significant relationship between the small basin's MOC weakening and its weakening heat storage rate in our set-up. Moreover, we find that the heat storage contrast between the two basins of DDrake remains almost constant during the period of MOC weakening, and throughout the rest of the simulated 200 years on decadal timescales.

Contrary to expectations, we find that the anomalous downward MOC heat flux $\Delta\mathcal{H}_{MOC}$ *increases* as the SB MOC weakens. Furthermore, by decomposing the MOC heat flux into MOC weakening and differential warming components (equation 2), we find that the dominant term is in fact from differential warming, with the control overturning playing a prominent role (figure 3a). Finally, although $\Delta\mathcal{H}_{MOC}$ increases, this does not lead to an increase in the heat storage contrast, as this additional heat input is subsequently lost to the southern ocean region (figure 3b). Thus, although the presence of a MOC is important for the small basin's enhanced heat storage rate, the change in MOC strength is surprisingly unimportant.

Our results underline the importance of the AMOC in ocean heat storage, and for its accurate representation in other, predictive climate models. Continued observational monitoring efforts such as RAPID (Smeed et al., 2018) and the Overturning in the Subpolar North Atlantic Program (OSNAP) (M. Lozier et al., 2019), in conjunction with more advanced high-resolution climate models, should drive a deeper understanding of the AMOC, but we also encourage the use of simpler, more conceptual models such as DDrake in order to make sense of this increasing complexity.

Acknowledgments

P.S. was supported by the UK Engineering and Physical Sciences Research Council (EPSRC) Centre for Doctoral Training in Mathematics of Planet Earth. The CMIP5 data used in this paper is available at the Earth System Grid Federation (ESGF) Portal (https://esgf-node.llnl.gov/search/cmip5/).

References

Armour, K. C., Marshall, J., Scott, J. R., Donohoe, A., & Newsom, E. R. (2016). Southern ocean warming delayed by circumpolar upwelling and equatorward transport. *Nature Geoscience*, *9*(7), 549.

Caesar, L., Rahmstorf, S., Robinson, A., Feulner, G., & Saba, V. (2018). Observed fingerprint of a weakening atlantic ocean overturning circulation. *Nature*, *556*(7700), 191.

Chen, X., & Tung, K.-K. (2014). Varying planetary heat sink led to global-warming slowdown and acceleration. *Science*, *345*(6199), 897–903.

Chen, X., & Tung, K.-K. (2018). Global surface warming enhanced by weak atlantic overturning circulation. *Nature*, *559*(7714), 387.

Desbruyeres, D., McDonagh, E. L., King, B. A., & Thierry, V. (2017). Global and full-depth ocean temperature trends during the early twenty-first century from argo and repeat hydrography. *Journal of Climate*, *30*(6), 1985–1997.

Drijfhout, S. S., Blaker, A. T., Josey, S. A., Nurser, A., Sinha, B., & Balmaseda, M. (2014). Surface warming hiatus caused by increased heat uptake across multiple ocean basins. *Geophysical Research Letters*, *41*(22), 7868–7874.

Ferreira, D., & Marshall, J. (2015). Freshwater transport in the coupled ocean-atmosphere system: a passive ocean. *Ocean Dynamics*, *65*(7), 1029–1036.

Ferreira, D., Marshall, J., Bitz, C. M., Solomon, S., & Plumb, A. (2015). Antarctic ocean and sea ice response to ozone depletion: A two-time-scale problem. *Journal of Climate*, *28*(3), 1206–1226.

Ferreira, D., Marshall, J., & Campin, J.-M. (2010). Localization of deep water formation: Role of atmospheric moisture transport and geometrical constraints on ocean circulation. *Journal of Climate*, *23*(6), 1456–1476.

Frölicher, T. L., Sarmiento, J. L., Paynter, D. J., Dunne, J. P., Krasting, J. P., & Winton, M. (2015). Dominance of the southern ocean in anthropogenic carbon and heat uptake in cmip5 models. *Journal of Climate*, *28*(2), 862–886.

Gent, P. R., & Mcwilliams, J. C. (1990). Isopycnal mixing in ocean circulation models. *Journal of Physical Oceanography*, *20*(1), 150–155.

Gregory, J., Dixon, K., Stouffer, R., Weaver, A., Driesschaert, E., Eby, M., ... others (2005). A model intercomparison of changes in the atlantic thermohaline circulation in response to increasing atmospheric co2 concentration. *Geophysical Research Letters*, *32*(12).

Hansen, J., Sato, M., Kharecha, P., & Schuckmann, K. v. (2011). Earth's energy imbalance and implications. *Atmospheric Chemistry and Physics*, *11*(24), 13421–13449.

Klinger, B. A., Marshall, J., & Send, U. (1996). Representation of convective plumes by vertical adjustment. *Journal of Geophysical Research: Oceans*, *101*(C8), 18175–18182.

Kostov, Y., Armour, K. C., & Marshall, J. (2014). Impact of the atlantic meridional overturning circulation on ocean heat storage and transient climate change. *Geophysical Research Letters*, *41*(6), 2108–2116.

Liu, W., Xie, S.-P., Liu, Z., & Zhu, J. (2017). Overlooked possibility of a collapsed atlantic meridional overturning circulation in warming climate. *Science Advances*, *3*(1), e1601666.

Lozier, M., Li, F., Bacon, S., Bahr, F., Bower, A., Cunningham, S., ... others (2019). A sea change in our view of overturning in the subpolar north atlantic. *Science*, *363*(6426), 516–521.

Lozier, M. S. (2012). Overturning in the north atlantic. *Annual review of marine science*, *4*, 291–315.

Marshall, J., Adcroft, A., Hill, C., Perelman, L., & Heisey, C. (1997). A finite-volume, incompressible navier stokes model for studies of the ocean on parallel computers. *Journal of Geophysical Research: Oceans*, *102*(C3), 5753–5766.

Marshall, J., Hill, C., Perelman, L., & Adcroft, A. (1997). Hydrostatic, quasi-hydrostatic, and nonhydrostatic ocean modeling. *Journal of Geophysical Research: Oceans*, *102*(C3), 5733–5752.

Marshall, J., Scott, J. R., Armour, K. C., Campin, J.-M., Kelley, M., & Romanou, A. (2015). The ocean's role in the transient response of climate to abrupt greenhouse gas forcing. *Climate Dynamics*, *44*(7-8), 2287–2299.

Meehl, G. A., Arblaster, J. M., Fasullo, J. T., Hu, A., & Trenberth, K. E. (2011). Model-based evidence of deep-ocean heat uptake during surface-temperature hiatus periods. *Nature Climate Change*, *1*(7), 360.

Molteni, F. (2003). Atmospheric simulations using a gcm with simplified physical parametrizations. i: Model climatology and variability in multi-decadal experiments. *Climate Dynamics*, *20*(2-3), 175–191.

Myhre, G., Highwood, E. J., Shine, K. P., & Stordal, F. (1998). New estimates of radiative forcing due to well mixed greenhouse gases. *Geophysical research letters*, *25*(14), 2715–2718.

Rahmstorf, S., Box, J. E., Feulner, G., Mann, M. E., Robinson, A., Rutherford, S., & Schaffernicht, E. J. (2015). Exceptional twentieth-century slowdown in atlantic ocean overturning circulation. *Nature climate change*, *5*(5), 475.

Redi, M. H. (1982). Oceanic isopycnal mixing by coordinate rotation. *Journal of Physical Oceanography*, *12*(10), 1154–1158.

Saenko, O. A., Yang, D., & Gregory, J. M. (2018). Impact of mesoscale eddy transfer on heat uptake in an eddy-parameterizing ocean model. *Journal of Climate*, *31*(20), 8589–8606.

Smeed, D., Josey, S., Beaulieu, C., Johns, W. E., Moat, B., Frajka-Williams, E., ... others (2018). The north atlantic ocean is in a state of reduced overturning. *Geophysical Research Letters*, *45*(3), 1527–1533.

Srokosz, M., & Bryden, H. (2015). Observing the atlantic meridional overturning circulation yields a decade of inevitable surprises. *Science*, *348*(6241), 1255575.

Stocker, T. (2014). *Climate change 2013: the physical science basis: Working group i contribution to the fifth assessment report of the intergovernmental panel on climate change*. Cambridge University Press.

Straneo, F. (2006). On the connection between dense water formation, overturning, and poleward heat transport in a convective basin. *Journal of Physical Oceanography*, *36*(9), 1822–1840.

Trenberth, K. E., Fasullo, J. T., & Balmaseda, M. A. (2014). Earth's energy imbalance. *Journal of Climate*, *27*(9), 3129–3144.

Von Schuckmann, K., Palmer, M., Trenberth, K., Cazenave, A., Chambers, D., Champollion, N., ... others (2016). An imperative to monitor earth's energy imbalance. *Nature Climate Change*, *6*(2), 138.

Watanabe, M., Kamae, Y., Yoshimori, M., Oka, A., Sato, M., Ishii, M., ... Kimoto, M. (2013). Strengthening of ocean heat uptake efficiency associated with the recent climate hiatus. *Geophysical Research Letters*, *40*(12), 3175–3179.

Weaver, A. J., Sedláček, J., Eby, M., Alexander, K., Crespin, E., Fichefet, T., ... others (2012). Stability of the atlantic meridional overturning circulation: A model intercomparison. *Geophysical Research Letters*, *39*(20).

Winton, M. (2000). A reformulated three-layer sea ice model. *Journal of atmospheric and oceanic technology*, *17*(4), 525–531.

Winton, M., Griffies, S. M., Samuels, B. L., Sarmiento, J. L., & Frölicher, T. L. (2013). Connecting changing ocean circulation with changing climate. *Journal of climate*, *26*(7), 2268–2278.

Xie, P., & Vallis, G. K. (2012). The passive and active nature of ocean heat uptake in idealized climate change experiments. *Climate Dynamics*, *38*(3-4), 667–684.

Zanna, L., Khatiwala, S., Gregory, J. M., Ison, J., & Heimbach, P. (2019). Global reconstruction of historical ocean heat storage and transport. *Proceedings of the National Academy of Sciences*, *116*(4), 1126–1131.

Zika, J. D., Sijp, W. P., & England, M. H. (2013). Vertical heat transport by ocean circulation and the role of mechanical and haline forcing. *Journal of Physical Oceanography*, *43*(10), 2095–2112.

Geophysical Research Letters

Supporting Information for

Ocean heat storage rate unaffected by MOC weakening in an idealised climate model

Peter Shatwell[1], Arnaud Czaja[1], David Ferreira[2]

[1]Department of Physics, Imperial College London; [2]Department of Meteorology, University of Reading

Contents of this file

Figures S1 to S3

Introduction

This document provides additional figures to clarify and support arguments presented in the paper.

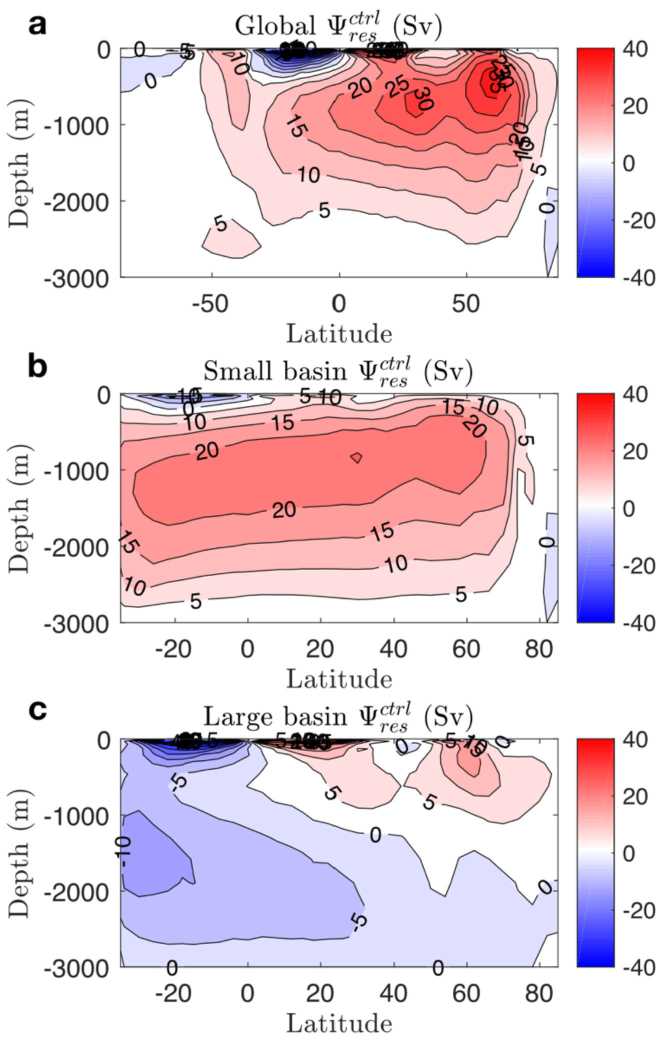

Figure S1. Control residual overturning streamfunctions for the (a) global, (b) small basin, and (c) large basin regions of DDrake (in Sv).

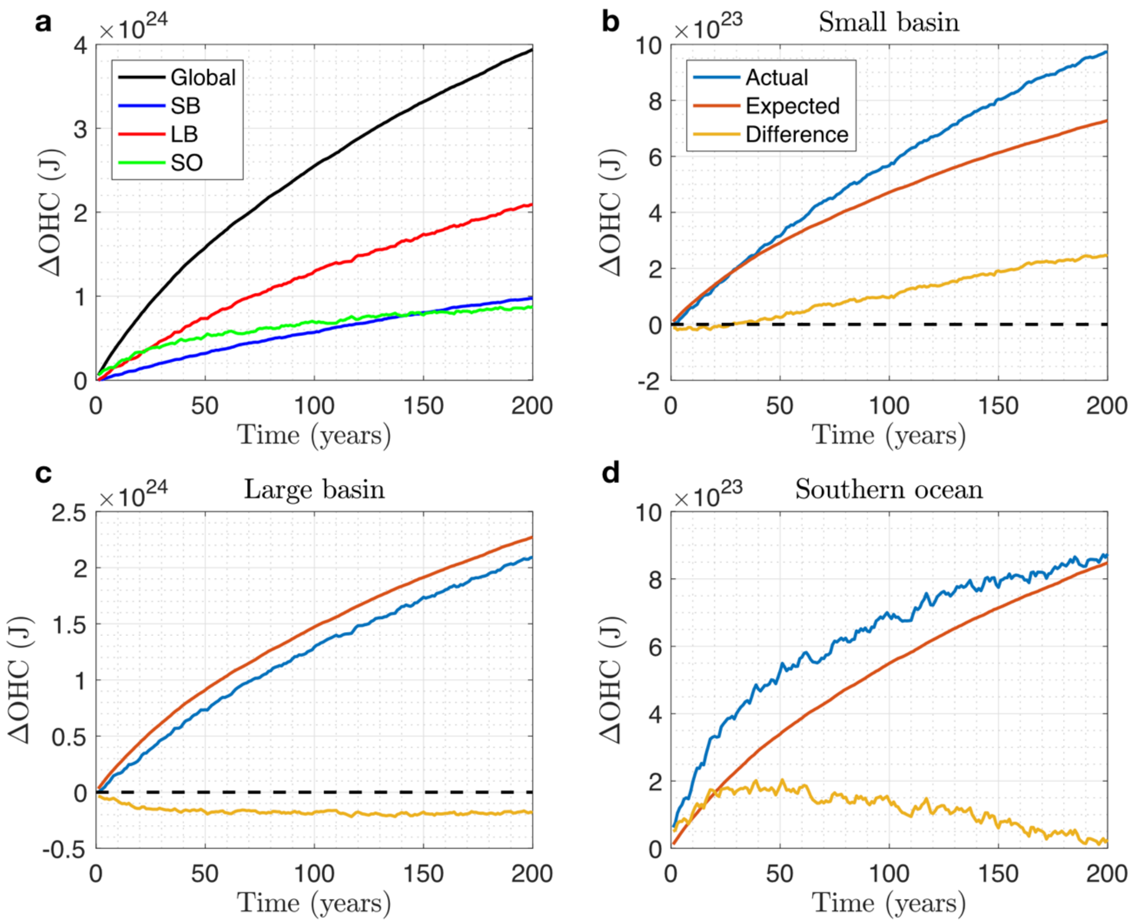

Figure S2. (a) Time-series of heat storage responses (in J) for all DDrake basins. (b-d) Comparison of actual versus expected heat storage responses (in J) considering the fractional coverage of the total surface area for (b) the small basin (SB), (c) the large basin (LB), and (d) the southern ocean (SO) of DDrake. For each basin B, the 'expected' curves are (B's surface-area/global surface-area)*(global response) i.e. the surface-area-weighted fraction of the black curve in (a). From this perspective, we see that the SB overperforms (while the LB underperforms) with respect to its size.

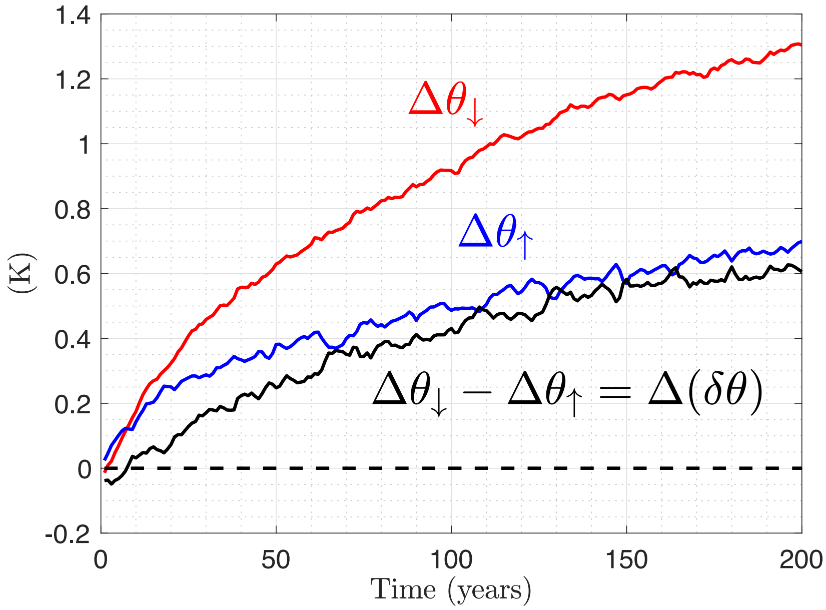

Figure S3. Time series of warming responses for the small basin MOC downwelling ($\theta_{\downarrow}$, red) and upwelling ($\theta_{\uparrow}$, blue) regions (as defined in the text), and their difference $\Delta(\delta\theta)$ (in K). The downwelling region warms at a faster rate than the upwelling region.